International Journal of Progressive Sciences and Technologies (IJPSAT)
ISSN: 2509-0119.

https://ijpsat.org/
Vol. 48 No. 1 December 2024, pp. 462-470

Wave Height Forecasting Technique In The Southern Part Of The Mozambique Channel

Elie Maka Remalay SAFIDY VALANTINO[1], Honoré RAZAFIMANDIMBY[2], Jacques Chrysologue RATSIMAVO[3], Adolphe Andriamanga RATIARISON[4]

[1,2,3]Laboratory of Atmospheric, Climate, and Ocean Dynamics - University of Toliara -

[4]Laboratory of Atmospheric, Climate, and Ocean Dynamics - University of Tananarive

Abstract – The southern part of the Mozambique Channel, subject to complex oceanic conditions with variable wave heights, poses challenges for navigation and economics activities such as fishing, which are essential for the communities in Southwest of Madagascar. This study proposes a model based on neural networks to forecast wave heights. By regionalizing the study area, this models enhances forecasting accuracy, contributing to maritime safety and risk management.

Keywords – Mozambique Channel, wave height, forecasting, neural network, maritime safety.

1. INTRODUCTION :

Many communities in Southwest of Madagascar relies on navigation and fishing in the southern Mozambique Channel, an area with complex weather conditions that make navigation risky. Unstable wave heights pose a challenge for maritime safety, particularly for local fishermen. This study focuses on this region (22°S to 29°S, 36°E to 43°E) and proposes a numerical model using neural networks for short-term wave height forecasting. The aim is to improve maritime safety and support economics activities such as fishing and tourisms.

2. METHODOLOGIES :

The wave height data used in this study are daily records collected over 40 years (from first January 1979 to December 31, 2018) from the ECMWF site. These data are structured into a three-dimensional matrix (latitude × longitude × days). The first step of the analysis involves calculating monthly climatological averages, followed by the application of area classification using the Kohonen network.

2.1. Regionalization via Kohonen Network

The self-organizing maps of Kohonen is a neural method developed by Teuvo Kohonen in 1982, used for automatic classification tasks. [ABLAYE, 2018]. This model belongs to the class of unsupervised neural networks, meaning that no human intervention is being required and minimal information is needed regarding the characteristics of the input data. Kohonen maps will discover relationships of which exist among the input data [HUGUES, 1998].

2.1.1. Monthly Climatological Average of Wave Heights:

The monthly climatological averages refer to the mean wave heights calculated for each month over a long period, providing a reference for climatic conditions for each month. These averages are used for classification using the Kohonen network.

$$\overline{X_{\iota\, moycl\iota m}} = \frac{1}{T}\sum_{1}^{T} X_i$$

T : total number of months during the period

X_i : value of the i-th series

$\overline{X_{\iota\, moycl\iota m}}$: climatological average

2.1.2. Kohonen Network Learning:

The learning rule for a neuron j belonging to the variable topological neighborhood of the winning neuron $i(x)$ describes a rotation of the weight vectors toward the input vector and is stated as follows:

$$\omega_j(n+1) = \begin{cases} \omega_j(n) + \eta(n)\left[x - \omega_j(n)\right] & ssi\ j \in \Lambda_{i(x)}(n) \\ \omega_j(n) & ssi\ j \notin \Lambda_{i(x)}(n) \end{cases}$$

$\Lambda_{i(x)}$: topological neighborhood around the winning neurons at discrete time

$n, \eta(n)$: neighborhood function that includes a learning rate function.

ω_j : synaptic weight vectors related to the output neuron

In the case of a Gaussian neighborhood function around the winning neurons $i(x), \eta(n)$is expressed as follows:

$$\eta(n) = \alpha(n).e^{-\frac{\left\|r_j - r_{i(x)}\right\|^2}{2\sigma(n)^2}} \quad , j \in \Lambda_{i(x)}(n)$$

$\left\|r_j - r_{i(x)}\right\|$: distance between neuron j and the winning neuron $i(x)$

$\alpha(n)$: adaptation rate of the neurons located within $\Lambda_{i(x)}(n)$.

International Journal of Progressive Sciences and Technologies (IJPSAT)
ISSN: 2509-0119.

https://ijpsat.org/
Vol. 48 No. 1 December 2024, pp. 462-470

2.2. Modeling and Forecasting Technique using Artificial Neural Networks

Modeling plays a crucial role in understanding and anticipating variations in climatic parameters such as wave heights by integrating historical wave height data from the past 40 years. We use feedforward neural networks because of their ability to model complex nonlinear relationships.

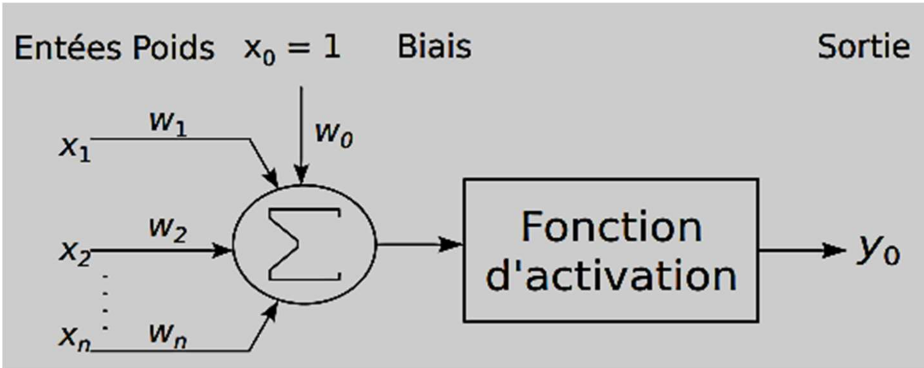

Figure 1: perceptron

w_i : Weights, x_i : A multiple input signal; w_0 : additional input or bias, y_0 : output signal

2.2.1. Data normalization::

It is a step that consists of transforming the data to bring them to the same scale, generally between « 0 and 1 » ou « -1 and 1 ».

$x' = \frac{x - x_{min}}{x_{max} - x_{min}}$, x' : normalized data;; x: raw data ;

x_{min} , x_{max} : the minimum and maximum values of the series;

2.2.2. Feedforward network architecture:

A feedforward neural network chains together different layers of neurons, each layer being a function of the previous one. If the input vector is $\boldsymbol{x} \in \mathbb{R}$, the first layer performs a linear or affine operation on x, then it computes a nonlinear function of the result:

$z = W^{[1]}x + b^{[1]}$ and then $a^{[1]} = g^{[1]}(z^{[1]})$ [***RIJA at al., 2022***].

$W^{[1]}$: first weight matrix of size $n^2 \times p$; $b^{[1]}$: offset vector of size $n^2 \times 1$

g^1 : activation function, generally nonlinear (when we write $g^{[1]}(z)$ it will be applied to all coordinates of z).

The k-th layer is then written as a function of the previous one:

$$a^{[k]} = g^{[k]}\left(W^{[k]}a^{[k-1]} + b^k\right)$$

$$z^{[k]} = W^{[k]}a^{[k-1]} + b^k$$

$W^{[k]}$: weight matrix of size $n^{[k+1]} \times n^{[k]}$; $b^{[k]}$: offset vector of size $n^{[k+1]} \times 1$, and so on, up to the output layer l.

$$\hat{y}(x, W, b) = g^{[l]}\left(W^{[l]}a^{[l-1]} + b'\right)$$

After generating the output signal from a normalized series, we proceed to denormalization to return into the original data scale.

International Journal of Progressive Sciences and Technologies (IJPSAT)
ISSN: 2509-0119.

https://ijpsat.org/
Vol. 48 No. 1 December 2024, pp. 462-470

- **Activation function :**

This is a function that establishes a non-linear relationship, giving the model more flexibility compared to linear regression [RANDRIANASOLO, 2023].

Table 1: Activation function

Activation function	Mathematical expression	Data scale
Sigmoïde	$\sigma(z) = \frac{1}{1+e^{-z}}$	[0,1]

3. RESULTS

3.1. Results of classification using the Kohonen network

The results obtained from the classification using the Kohonen network show a segmentation of the data into three classes ***(fig.2)***. The neurons organized themselves into clusters corresponding to similar wave height conditions in each of the studied areas. To distinguish the three sub-areas, they need to be named and colored : ***zone A*** is colored yellow, ***zone B*** is in green, and ***zone C*** is in red.

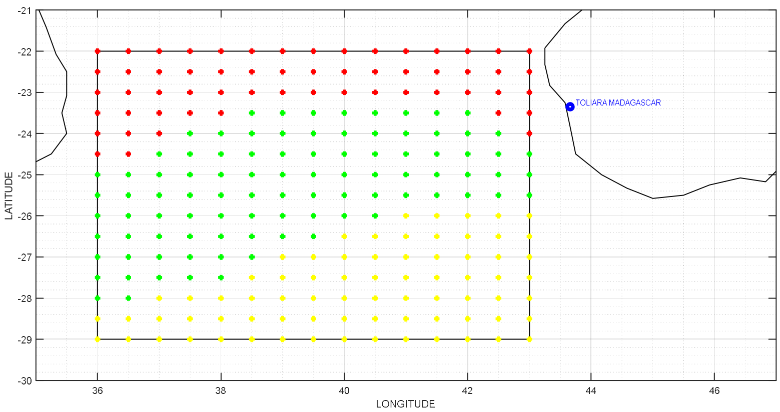

Figure 2: Classification by zone according to similarities in wave heights

3.2. Modelling result

The results obtained show that the neural network model accurately predicts the wave height for three study areas. The figures below show all the signs of the models performance.

3.2.1. Hyperparameter Adjustment

The fixed "Lag" at 5 indicates that the previous 5 periods are considered uniformly informative for prediction in each area, suggesting a common temporal dynamic. zones A and C, requiring a larger hidden layer, suggest a more complex data structure requiring a deeper model for better generalization. zone B, with fewer neurons, requires a less complex model that generalizes better, despite slightly lower training performance.

International Journal of Progressive Sciences and Technologies (IJPSAT)
ISSN: 2509-0119.

https://ijpsat.org/

SCHOLAR AI Be Smart

Vol. 48 No. 1 December 2024, pp. 462-470

Table 2: Hyperparameter

	Lag	*hiddenLayerSize*	*Train*	*Validation*	*Test*
zone A	5	35	78%	11%	11%
zone B	5	18	73%	12%	15%
Zone C	5	35	80%	9%	11%

3.2.2. Mean squared error

For ***zone A*** (fig. 3), training over 9 epochs shows a stabilization of the validation error starting from epoch 3, indicating good generalization, with the best validation performance at 0.030495 and a low discrepancy with the test error. For ***zone B*** (fig. 4), the model achieves its best performance at epoch 11 with a MSE of 0.03444 in validation and a stable test error, confirming its accuracy. ***Zone C*** (fig. 5) shows a rapid stabilization of the error starting from epoch 4, with a MSE of 0.019483 in validation, also reflecting good generalization.

Zone A	**Zone B**	**Zone C**
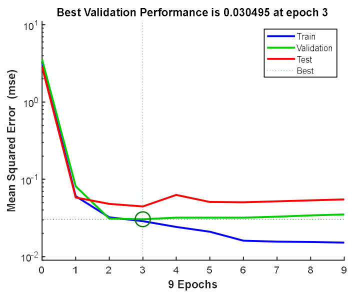 *Figure 3: Quadratic error-zone A*	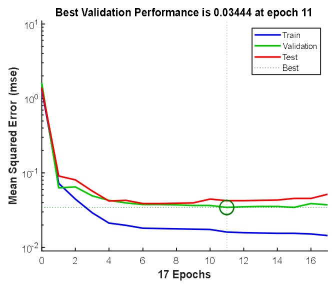 *Figure 4: Quadratic error -zone B*	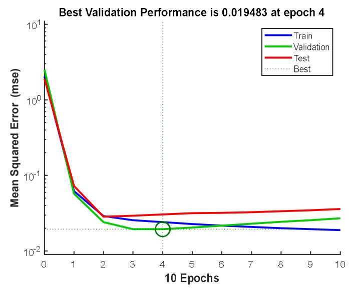 *Figure 5: Quadratic error -zone C*

3.2.3. Comparison of Model Targets, Outputs and Errors as a Function of Time

Figures 6, 7, and 8 show that the models of the three zones (zone A, zone B, zone C) generally follow the trends of the time series, with low and random prediction errors, although they struggle to predict certain abrupt variations. The histograms presented in figures 9, 10, and 11 illustrate the error distributions for each zone, which are mostly concentrated around zero, indicating overall fairly accurate predictions despite some extreme errors. Overall, the model captures the general trends of the time series well, with generally small errors.

International Journal of Progressive Sciences and Technologies (IJPSAT)
ISSN: 2509-0119.

https://ijpsat.org/
Vol. 48 No. 1 December 2024, pp. 462-470

Zone A	Zone B	Zone C
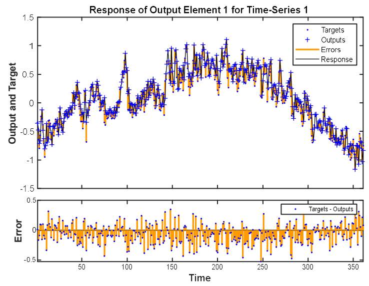 *Figure 6:network quality-zone A*	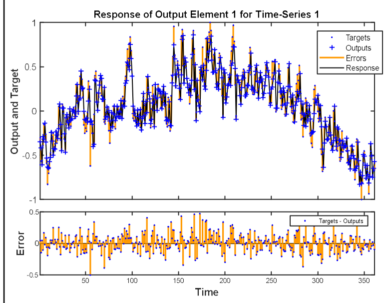 *Figure 7: network quality -zone B*	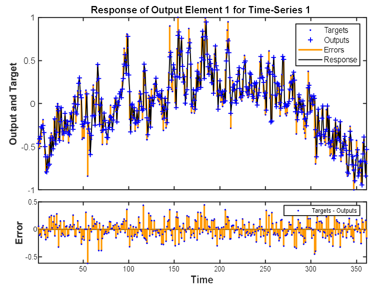 *Figure 8: network quality -zone C*
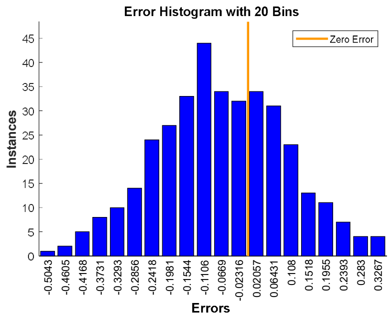 *Figure 9:Error histogram-A*	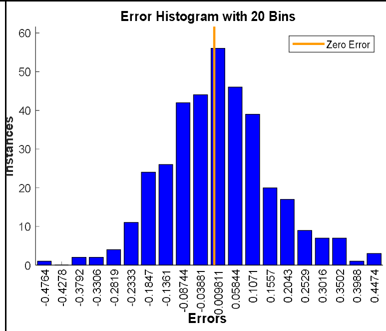 *Figure 10: Error histogram -B*	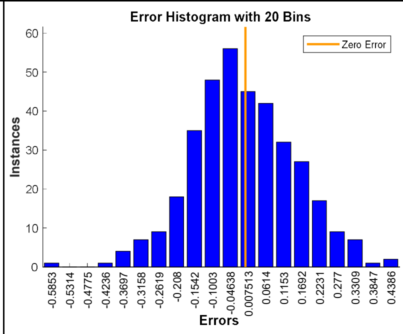 *Figure 11: Error histogram -C*

3.2.4. Neural Network Regression Model

The regression lines (fig. 12, fig.13, fig. 14) show strong correlations (> 0.90) between predicted and actual values for the training, validation, and test sets, indicating that the model captures the trends in the data well. Points close to the diagonal line demonstrate good performance, with a correlation coefficient R close to 1, indicating a strong linear relationship. The results for the three areas confirm that the regression models are very effective across the entire dataset, with excellent generalization. The high **R** values and the linear relationship described by an equation suggest a precise, regularized, and reliable model for prediction.

International Journal of Progressive Sciences and Technologies (IJPSAT)
ISSN: 2509-0119.

https://ijpsat.org/
Vol. 48 No. 1 December 2024, pp. 462-470

Zone A	Zone B	Zone C
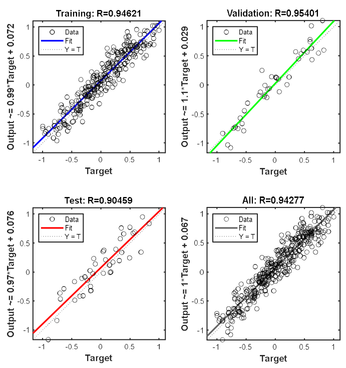 *Figure 12: regression model -A*	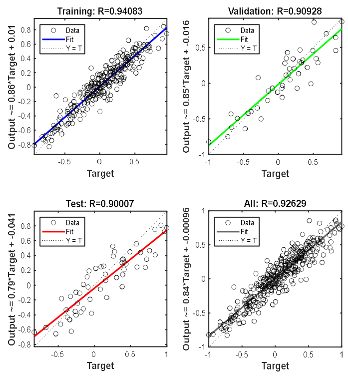 *Figure 13: regression model -B*	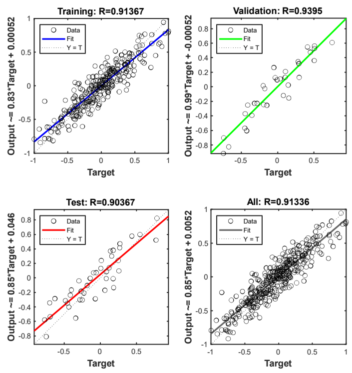 *Figure 14: regression model -C*

3.3. Résultat de prévision

Zone A **:** the Figure 15 and Table 3 present the forecast and observed wave heights for the first 10 days of a year, along with the corresponding deviations. The deviations are low, ranging from 0.02 m to 0.30 m. This indicates that the models predict the data with high accuracy.

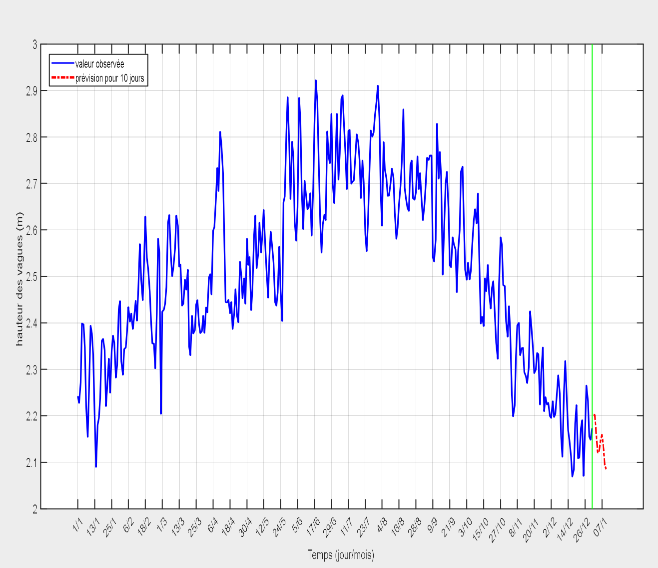

Figure 15: 10-day forecast-zone A

Table 3: Comparison between Observation and Forecast (denormalized values)

Observation		forecast	deviation
1er Jan	2,242	2,201	0,042
2 Jan	2,228	2,201	0,069
3 Jan	2,271	2,159	0,112
4 Jan	2,399	2,121	0,278
5 Jan	2,396	2,122	0,274
6 Jan	2,348	2,148	0,200
7 Jan	2,221	2,160	0,061
8 Jan	2,155	2,135	0,020
9 Jan	2,254	2,094	0,160
10 Jan	2,394	2,085	0,309

Zone B : the figure 16 and Table 4 show the results of the wave height forecasts for zone B. The neural network model generally follows the variations of the observed data, with forecasts typically lower than the observations. The discrepancies range from 0.014 m (January 7) to 0.233 m (January 5), indicating good accuracy on some days, but larger errors on others. The general trend is well captured by the forecasts.

International Journal of Progressive Sciences and Technologies (IJPSAT)
ISSN: 2509-0119.

https://ijpsat.org/
Vol. 48 No. 1 December 2024, pp. 462-470

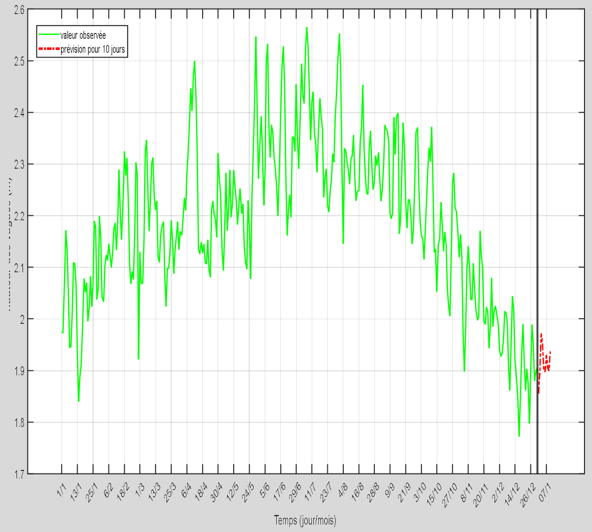

Figure 16: 10-day forecast - zone B

Table 4: Comparison between Observation and Forecast (denormalized values)

Observation		forecast	deviation
1er Jan	1,974	1,855	0,119
2 Jan	1,973	1,900	0,073
3 Jan	2,076	1,971	0,105
4 Jan	2,171	1,953	0,218
5 Jan	2,134	1,901	0,233
6 Jan	2,048	1,898	0,150
7 Jan	1,944	1,930	0,014
8 Jan	1,946	1,906	0,040
9 Jan	2,012	1,900	0,112
10 Jan	2,109	1,937	0,172

Zone C : The differences between observations and forecasts range from 0.028 m to 0.216 m (*Table* 5). This indicates that the model is more accurate on some days than others. The forecasting errors are generally small, but certain values (such as those from January 4 and January 5) show the largest discrepancies, suggesting that the model might struggle to capture certain peaks or more sudden variations in the wave height data. The neural network model (*figure* 17) correctly predicts the general trend of wave heights, but it is sometimes exhibits significant errors, particularly for specific days.

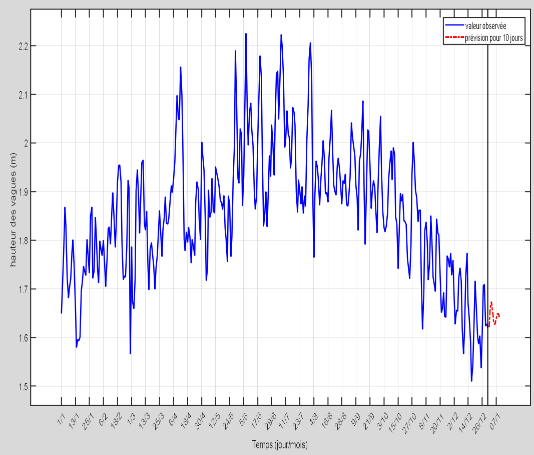

Figure 17 : 10-day forecast - zone C

Table 5: Comparison between Observation and Forecast (denormalized values)

Observation		forecast	deviation
1er Jan	1,649	1,621	0,028
2 Jan	1,701	1,663	0,038
3 Jan	1,776	1,673	0,103
4 Jan	1,868	1 ,652	0,216
5 Jan	1,827	1,630	0,197
6 Jan	1,722	1,627	0,095
7 Jan	1,682	1,637	0,045
8 Jan	1,702	1,648	0,054
9 Jan	1,721	1,649	0,072
10 Jan	1,777	1,640	0,137

4. DISCUSSION

The linear regression results of this study, with R^2 values ranging from 0.62 to 0.75 and RMSE between 8% and 11.89%, are similar to other research such as the Chawla et al. (2013), demonstrating the model's effectiveness in complex maritime environments. Compared to Kamranzad et al. (2011) and Kazeminezhad et al. (2005), our model shows the best performance and higher accuracy. The efficiency of neural networks is confirmed by the low MSE in all three zones, thanks to optimized hyperparameter tuning. The rapid stabilization of error from the early epochs of training, consist with Hsieh's observations (2009), validates the robustness of our model. It achieves performance comparable to that of Shamshirband et al. (2020), with R^2 values exceeding 0.90.

5. CONCLUSION

The model's training shows a good generalization across the three zones. Zone A stabilizes its error at epoch 3 with an MSE of 0.030495, Zone B reaches its best performance at epoch 11 with an MSE of 0.03444, and Zone C stabilizes quickly at epoch 4 with an MSE of 0.019483. The regressions show high correlations ($R > 0.90$) between the actual and predicted values. The errors are concentrated around zero, indicating a good model accuracy. The discrepancies between observations and forecasts are small, further demonstrating the model's accuracy, suggesting that the model generally predicts well, except for certain sudden variations.

REFERENCES

[1]. ARUN Chawla, DEANNA M. SPINDLER, HENDRICK L. Tolman (2013). Validation of a thirty-year wave hindcast using the Climate Forecast System Reanalysis winds. Ocean Modelling, ARTICLE. Volume 70, pages 189-206.

[2]. FAYE Ablayé, 2018.Cartes topologiques de Kohonen. Article sur le journal meritis.

[3]. HUGUES Bélanger,1998. Réseau de Kohonen pour la détection des contours d'objets dans une images à niveaux des gris. MAITRISE. Ecole de Technologies Supérieure à l'université de Québec.

[4]. KAMRANZAD B. & ETEMAD-SHAHIDI A. & KAZEMINEZHAD M. H.2011. Wave height forecasting in the Persian Gulf. ARTICLE. Ocean Engineering, 38(1), 248–255.

[5]. KAZEMINEZHAD M. H., & ETEMAD-SHAHIDI A. (2005). Application of fuzzy inference system in the prediction of wave parameters. ARTICLE. *Ocean Engineering*, 32, 1709-1725.

[6]. RANDRIANARISOLO Tokiniaina Victoriot, 2023. Optimisation de l'écoulement de puissance dans un réseau électrique à l'aide de prédiction de charges en utilisant un réseau de neurone LSTM. MASTER. Université d'Antananarivo.

[7]. WILLIAM W. Hsieh, 2009. Machine learning methods in the environnemental sciences. ARTICLE. Cambridge University Press.